Optical and Quantum Electronics (2023) 55:1025
https://doi.org/10.1007/s11082-023-05362-y

Fabrication, structure, physical properties and FTIR spectroscopy of zirconate doped-borophosphate bioglasses

Hanan Al-Ghamdi[1] · Norah A. M. Alsaif[1] · F. Afaneh[2] · Z. Y. Khattari[2] · A. M. Abdelghany[3] · Y. S. Rammah[4]

Received: 21 June 2023 / Accepted: 30 August 2023 / Published online: 20 September 2023

Abstract

Samples of base calcium sodium borophosphate bioglasses doped with different amounts of zirconium oxide (ZrO_2) were prepared via melt quenching technique. Synthesized samples of nominal composition $xZrO_2$-$45B_2O_3$-(24.5-x)CaO-$24.5NaO_2$-$6P_2O_5$ x = 0 (S0)—5 (S6) mol% was investigated using fourier transforms infrared (FTIR) spectroscopy and deconvolution analysis technique (DAT) was employed to investigate the variation of the four coordinated borons. X-ray diffraction (XRD) technique to approve the isotropic character of the prepared glasses. Density (ρ) of samples varied from 2.606 g/cm^3 to 2.642 g/cm^3 and molar volume (V_m) enhanced from 25.565 cm^3.mol^{-1} to 26.649 cm^3.mol^{-1}. FTIR spectroscopy revealed that only reliable bands were considered and the (r^2-value) of the regression was nearly 0.99. The maximum value of the difference between experimental and theoretical data not exceeds ± 0.015 from the normalized spectral data. The fraction of the four coordinated boron was slightly changed due to the addition of ZrO_2 in the doping level. The decrease in the N4 values can be attributed to the structural changes combined with the conversion of BO4 to BO3 units.

Keywords Boron bioglasses · Zirconium oxide · XRD · FTIR

1 Introduction

The biomedical applications of glasses and glass–ceramic materials have received increased attention since Hench et. invention's of bioglass in 1971 (Hench et al. 1971). Due to their biocompatibility and strong interaction with bone, these materials are widely used for biomedical purposes as orthopaedic implant and bone filler materials (Salinas et al. 2000; Hench 1993). Moreover, bioactive glass–ceramics play a significant role in the biomedical application because of their peculiar microstructure, greater mechanical strength compared to derived glass, and superior thermal conductivity (Hench 1993, 1991; Baino et al. 2016). Furthermore, by allowing healthy tissue to grow on their surface through a layer of biologically active hydroxycarbonate apatite, they are capable of forming a direct link with the living bone without the development of surrounding fibrous tissue (HCA). The HCA phase that forms on the bioactive glass–ceramic surfaces is chemically and

Extended author information available on the last page of the article physically similar to the mineral phase of bone. This correlation plays a significant part in establishing an interfacial connection between bone and bioactive substance (Hoppe et al. 2011).

Abo-Mosallam and Mahdy (Montazerian and Dutra Zanotto 2016) reported on the crystallisation characteristics of glasses with various amounts of fluorocanasite and lithium disilicate. They came to the conclusion that flurocanasite and lithium disilicate glass–ceramics have potential use in dental application. The degradation and biocompatibility characteristics of the Na-Ca-phosphate and fluorapatite mixture in wollastonite-diopside glass–ceramic were studied by Mahdy et al. (Abo-Mosallam and Mahdy 2019).

Boron oxide (B_2O_3) is the most common oxide that can be applied as a glass basis. Borate-based glasses have a number of physical and chemical advantages, including a low melting point and high transparency (Mahdy et al. 2021; Kirdsiri et al. 2009). Khattari et al. (Yasaka et al. 2014) reported that the insertion of ZrO_2 in borate glasses structure leads to enhance their mechanical and optical properties. The insertion of rare earth ions such as Dy_2O_3, Sm_2O_3, and Nb_2O_3 into glass structures enhance their luminescence, physical, elastic, optical, and gamma ray shielding properties (Khattari et al. 2023; Divina et al. 2021; Bassam et al. 2023).

The use of borate glasses in biological applications is currently the subject of in-depth research (Arunkumar et al. 2023) as a result of the investigations conducted by Day et al. (M. Ottomeyer1 et al. 2016; Day et al. 2003; Huang et al. 2006; Brown et al. 2009). Because they are less chemically durable, borate glasses have the potential to be bioactive. These glasses can convert to hydroxyapatite (HA) partially or entirely more quickly thanks to the presence of borate in them. The osteogenic effects of borate on bone, namely on trabecular and alveolar type bone formation and maintenance, have already been demonstrated by many investigators and researchers working on bioactive glasses (Jia et al. 2010; Nielsen and Meacham 2011).

Krishnamacharyulu et al. (Gallardo-Williams et al. 2003) studied the physical properties of B_2O_3- SiO_2- P_2O_5- Na_2O- CaO doped with Ag_2O as bioglass systems for biomedical applications. They claimed that the increase of silver concentration leaads to enhance the capacity of formation of hydroxyapatite (HA) layer on the surface of the samples. Kamal (Krishnamacharyulu et al. 2018) reported on physical and structure features of Ag_2O-B_2O_3 bioactive glasses. Abo-Naf et al. (Kamal 2014) examined the structure and mechanical properties of Na_2O–CaO–B_2O_3–P_2O_5 glasses, they concluded the mentioned glasses can be applied as bioactive glasses. Abdelghany et al. (Abo-Naf et al. 2015) proved that the zinc-borate glasses and glass–ceramics were promising biomedical materials. Herein, bioactive glass samples of zirconium doped Hench bioglass (ZrO_2-B_2O_3-CaO-NaO_2-P_2O_5) have been fabricated. The structure, physical characteristics, and FTIR spectroscopy of the fabricated bioactive glasses have been investigated.

2 Experimental work

2.1 Sample preparation

Bioglass samples of nominal composition $xZrO_2$-$45B_2O_3$-(24.5-x)CaO-$24.5NaO_2$-$6P_2O_5$: $x = 0–5$ mol% were prepared using melt quenching technique. Analytical grade zirconium oxide used as received while calcium and sodium oxide was obtained from their carbonate partner. Ammonium dihydrogen phosphate and orthoboric acid was used as a source of phosphorus pentaoxide and boron oxide respectively. Weighted batches were put in porcelain crucible and sintered at 450 °C to remove carbonate, ammonia, and water. Temperature of the oven was raised gradually to 1200–1300 °C depending on glass composition. Obtained melts were swirled many times to obtain bubble free samples. The melts were then poured into stainless steel molds of required dimensions. Table 1 reveals sample nomination and composition.

2.2 Measurements

X-ray diffraction scans on a Cu K target with a secondary monochromator wave were performed using a PANalytical XPert PRO XRD system (where $\lambda = 1.540$ and the tube operated at 45 kV-40 mA) (Holland).

Density of the samples was measured using Archimedes principle adopting Xylene of density (0.868 g/cm^3) as bayonet fluid.

Fourier Transforms Infrared (FTIR) spectral data was recorded using Nicolet is10 Thermo Fischer Co. within the range extended between (4000–400 cm^{-1}) adopting 64 scans with resolution 2 cm^{-1}.

3 Results and discussion

3.1 Sample nature

Figure 1 illustrates a photo of the prepared bio-glass samples in this work. The mentioned photo confirms that all prepared samples are clear, transparent, and free of bubbles.

Figure 2 reveals the XRD pattern of the S0, S1, S2, S4, S5, and S6 borate bio-glasses containing variable amounts of zirconium oxide measured within Bragg's angle extended between 5–70 degrees. The obtained pattern characterized by a broad hallow centered at about 25 degree characterize the non-crystalline of all prepared samples and pointing to the isotropic nature of the glasses.

Table 1 Samples code, chemical composition, density, and molar volume of the prepared samples in (mol%)

Sample code	Chemical composition in mol%					Density, ρ (g/cm^3) ± 0.001	Molar volume, Vm (cm^3/mol) ± 0.001
	ZrO_2	CaO	NaO_2	P_2O_5	B_2O_3		
S0	0.0	24.5	24.5	6.0	45	2.606	25.565
S1	0.5	24	24.5	6.0	45	2.615	25.772
S2	1.0	23.5	24.5	6.0	45	2.618	25.910
S3	2.0	22.5	24.5	6.0	45	2.622	26.085
S4	3.0	21.5	24.5	6.0	45	2.632	26.248
S5	4.0	20.5	24.5	6.0	45	2.637	26.512
S6	5.0	19.5	24.5	6.0	45	2.642	26.649

Fig. 1 A photo of the prepared borate bioglasses

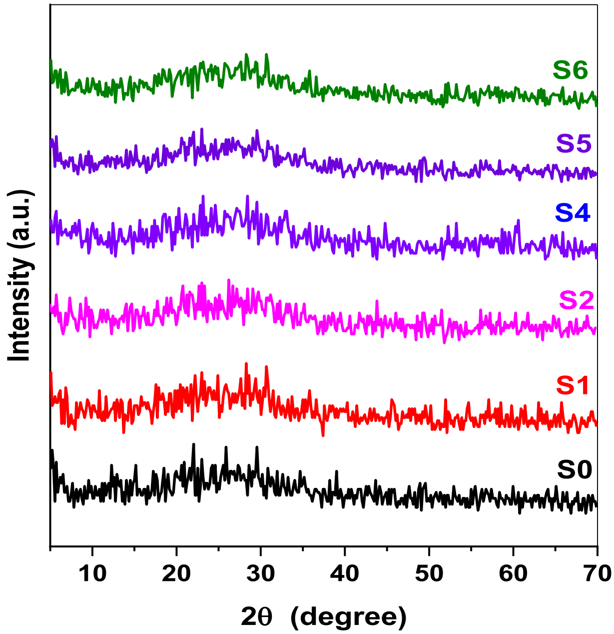

Fig. 2 XRD pattern of the S0, S1, S2, S4, S5, and S6 prepared borate bioglasses

3.2 Physical characteristics

Table 1 and Fig. 3 depicts the measured densities (ρ) of the prepared born bio-glasses (S0-S6). Results reveal that (ρ) was ranged of values between 2.606 g/cm^3 and 2.642 g/cm^3. Also, molar volume (V_m) of the proposed samples was varied from 25.565 $cm^3.mol^{-1}$ to 26.649 $cm^3.mol^{-1}$. As shown in Table 1 and Fig. 3, results of (ρ) and (V_m) indicate an increase in the same order. This may be attribute to the presence of heavy components such as P_2O_5 and Na_2O_2 in the glass networks may be partially responsible for this trend (Abo-Naf et al. 2015). The substitution of CaO with low density (3.34 $g.cm^{-3}$) by ZrO_2 with higher density (5.68 $g.cm^{-3}$), may also contribute to the observed increase in physical quantities. In addition, the enhancement in the ρ and V_m of S0-S6 samples can be ascribed to the greater molecular weight of ZrO_2 when compared to sodium oxide and the increase

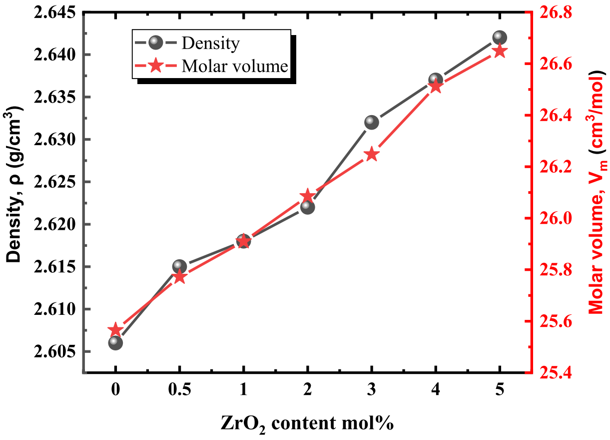

Fig. 3 Density (ρ) and molar volume (V_m) as a function of ZrO_2 content of the prepared borate bioglasses

in oxygen atoms in the mixture. These observations indicate that the glass network has become more open with a less dense structure (Abdelghany et al. 2014; El-Batal 2008).

3.3 FTIR spectroscopy

Figure 4 shows the FTIR spectrum data of the prepared glasses in the range 4000–400 cm^{-1}. Around 3434 cm^{-1}, the broad band resembling a water molecule was seen and was attributed to the O–H stretching vibrational modes. While the band at 1200–1600 cm^{-1} BO

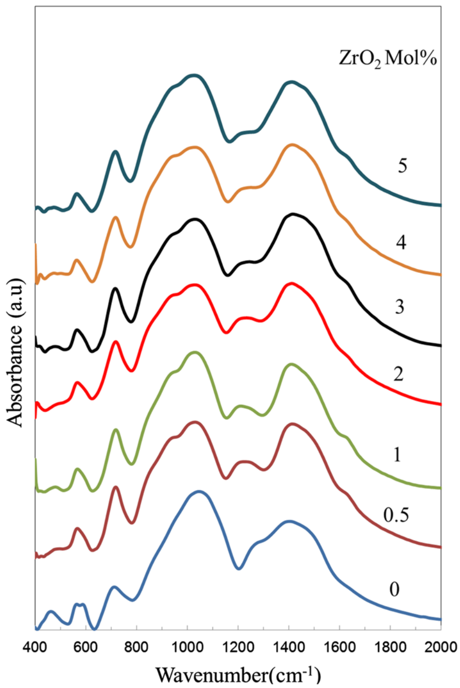

Fig. 4 FTIR spectral data within the region 4000–400 cm^{-1} of the prepared bioglasses

stretching vibrations and the peak seen at 930–1197 cm^{-1} BO tensile and stretching vibrations, respectively, of the trigonal BO-3 units of the tetrahedral (BO–4) units. Correlated with 700–720 cm^{-1} was the borate network's B-O-B bond bending. The P–O–B function group is represented by the band at 1228 cm^{-1}. The cation modifier is identified by the band at 400–600 cm^{-1}.

The BO_3 and BO_4 peaks relative areas were integrated to calculate the N4 using the next formula:

$$N_4 = \frac{BO_4}{BO_4 + BO_3} \tag{1}$$

Figure 5a and b shows the deconvoluted spectral data of the base bioglass sample (0 ZrO_2) and the variation of residuals within the studied spectral range. Figure 6a and b shows the deconvoluted spectral data of the S2 bioglass sample (1 mol% ZrO_2) and the variation of residuals within the studied spectral range. It was noticed that only reliable bands were considered and the (r^2-value) of the regression was nearly 0.99. In addition, the maximum value of the difference between experimental and theoretical data not exceeds ± 0.015 from the normalized spectral data.

To calculate the influence of BO4 on the change in the relative population of tetrahedral units BO4 and triangular units BO3, Fig. 7 plots the N4 as a function of BO4 concentration.

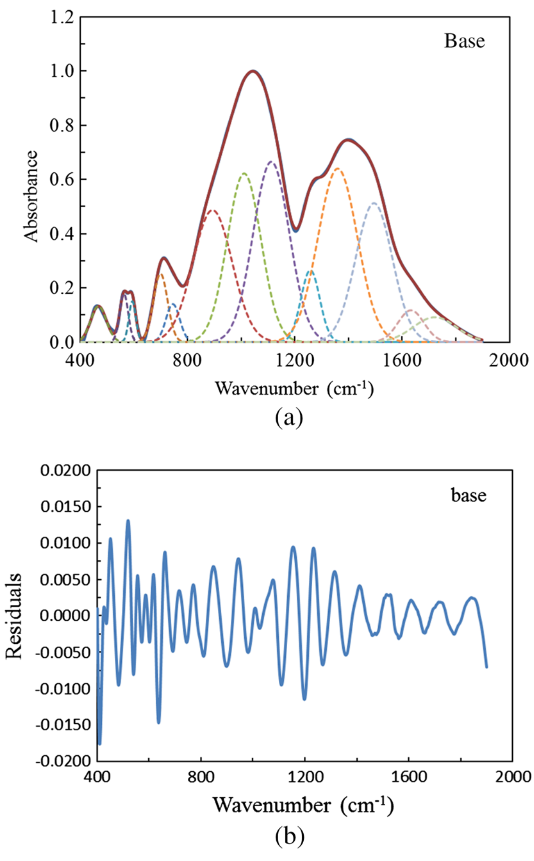

Fig. 5 **a** Deconvoluted spectral data of the base sample; **b** Variation of residuals of the base sample within the studied spectral range

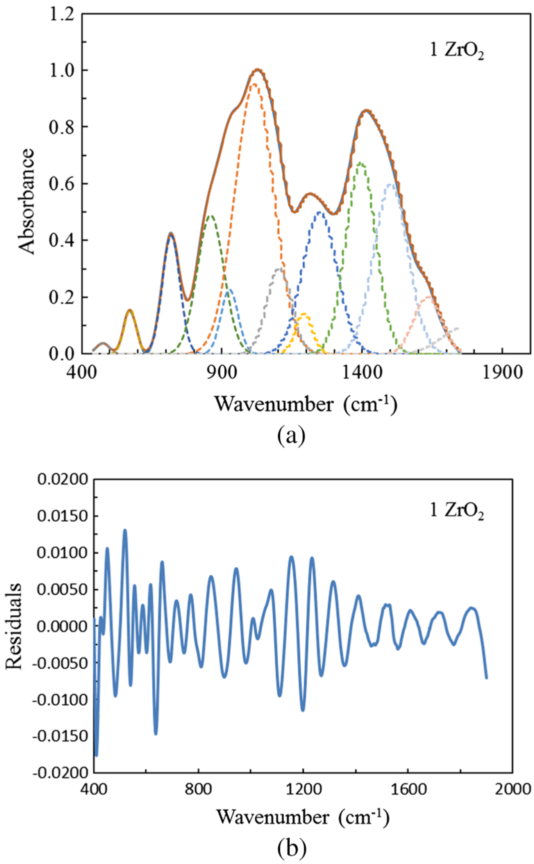

Fig. 6 **a** Deconvoluted spectral data of the S2 sample; **b** Variation of residuals of the S2 sample within the studied spectral range

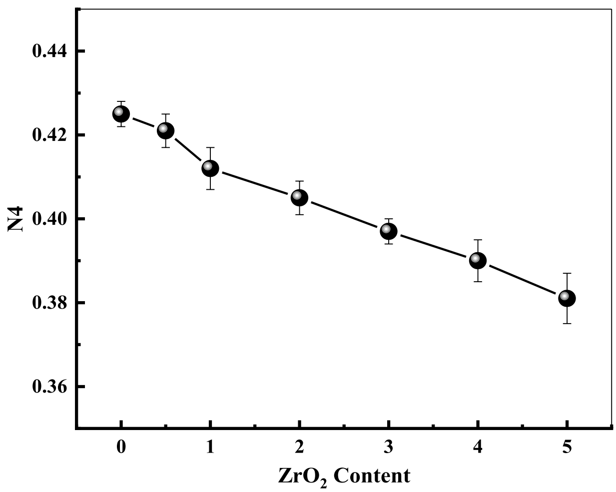

Fig. 7 The N4 as a function of ZrO_2 content in the fabricated bioglasses

The levels of N4 were found to vary depending on the BO4 concentration. It would seem that the presence of BO3 tends to reduce the number of BO4 units.

The presence of BO_3 and BO_4 structural groups was combined with the appearance of specific peaks within the FTIR spectra of the studied glasses related to such vibrational groups that are usually overlapped leading to the smearing of the less intense peaks.

Gaussian convolutions can be observed in the studied FTIR spectral data in the form of broadening or shoulders in descending lopes. The inverse problem, deconvolution of such data can help in understanding the structural variation resulting from the change in the composition of the studied glassy sample for specific applications. Spectral bands are usually considered as multiple overlapping Gaussian peaks where their sum can correlate with the experimental measured one. The suggestion of the number and position of the convoluted peaks based both on previously analyzed spectral data of similar glasses containing nearly similar forming oxides presented in literature and/or the second derivative of the experimental normalized FTIR data after corrections for background and dark current noises (Goel et al. 2008; Abdelghany 2010). Some authors (Abdelghany and Behairy 2020; Moustafa et al. 1994; Hammad et al. 2016) suggest too many peaks to calculate the relative area of each broad band based on statistical measures representing the proportion of the variance of dependent variables correlated with independent on in the regression model (R-squared or r^2) which are considered inaccurate. The examined parameters of all detected peaks using Gaussian deconvoluted for S1-S6 samples are tabulated in Table 2.

In addition, it was observed that the fraction of the four coordinated boron was slightly changed due to the addition of the zirconium oxide in the doping level. The decrease in the N4 values can be attributed to the structural changes combined with the conversion of BO4 to BO3 units. Such changes are usually combined with destroying BO4 units that may be converted to either BO_3 or/and BO_2O^- units with the generation of non-bridging oxygens. Therefore, the addition of zirconium (ZrO_2) ions in such glass appears to influence the glass network neighboring BO3 and zirconium cation which leads to the formation of both

Table 2 Parameters of deconvoluted bands of S1-S6 bioglasses

Sample	S1		S2		S3		S4		S5		S6	
Peak no	Center	R.A	Center	R.A	Center	R.A	Center	R.A	Center	R.A	Center	R.A
1	–	–	571.80	0.16	573.14	0.17	570.60	0.16	568.85	0.16	571.89	0.20
2	714.58	0.05	716.00	0.43	716.68	0.48	716.01	0.46	712.83	0.47	716.93	0.50
3	863.05	0.10	847.45	0.37	837.20	0.44	836.88	0.36	852.90	0.62	850.05	0.55
4	933.07	0.04	944.54	0.69	917.40	0.60	919.83	0.54	927.25	0.47	924.00	0.44
5	1027.98	0.29	1054.88	0.83	1026.75	0.92	1049.14	0.95	1009.17	0.89	1016.85	0.95
6	1131.07	0.10	–	–	1111.46	0.32	–	–	1090.25	0.43	1100.72	0.38
7	–	–	–	–	1188.46	0.25	–	–	–	–	1198.56	0.58
8	1262.68	0.09	1227.54	0.59	1249.03	0.59	1225.78	0.47	1223.01	0.65	1272.69	0.38
9	1335.73	0.06	1388.34	0.62	1393.43	0.89	1382.26	0.85	1393.40	0.79	1382.80	0.73
10	1374.71	0.06	–	–	–	–	–	–	–	–	–	–
11	1466.77	0.16	1495.00	0.68	–	–	–	–	–	–	1499.50	0.71
12	1591.63	0.05	–	–	1502.85	0.57	1513.83	0.60	1511.40	0.66	–	–
13	–	–	1629.70	0.22	1609.75	0.29	1634.12	0.11	1632.10	0.20	1630.92	0.14
14	–	–	–	–	–	–	1679.27	0.23	–	–	1691.08	0.18
15	–	–	1728.46	0.11	1736.21	0.14	570.60	0.16	1721.54	0.15	–	–

BO3 and ZrO4 structural groups. Such changes can be correlated with minor changes in both density and molar volume as shown in Table 1 and Fig. 3.

4 Conclusion

In this study, the direct influence of zirconate oxde (ZrO_2) on structure, density, molar volume, and FTIR spectroscopy of fabricated Hench bioglasses has been examined. The fabricated bioglass samples had the nominal composition xZrO_2-45B_2O_3-(24.5-x)CaO-24.5NaO_2-6P_2O_5, where x = 0–5 mol% and prepared via the melt quenching route. Fabricated bioglasses were coded as S0, S1, S2, S3, S4, S5, and S6 corresponding to x values. The amorphous nature of the prepared bioglasses proved via XRD measurements. Density (ρ) of samples was changed from 2.606 g/cm^3 and 2.642 g/cm^3 and molar volume (V_m) was varied from 25.565 cm^3.mol^{-1} to 26.649 cm^3.mol^{-1}. Only trustworthy bands were taken into account, according to FTIR spectroscopy, and the regression's (r^2-value) was close to 0.99. In terms of normalized spectral data, the maximum value of the discrepancy between experimental and theoretical data is limited at 0.015. The addition of ZrO_2 to the doping level slightly altered the proportion of the four coordinated boron. The structural modifications and the conversion of BO4 to BO3 units are to blame for the fall in N4 values.

Acknowledgements The authors express their gratitude to Princess Nourah bint Abdulrahman University Researchers Supporting Project number (PNURSP2023R28), Princess Nourah bint Abdulrahman University, Riyadh, Saudi Arabia.

Author contributions HA: Assisted in data collection & analysis and rearranging the manuscript first draft; NAMA: Conceptualization, review & editing, writing manuscript first draft; FA: Assisted in data analysis; ZYK: Assisted in data analysis and drawing the figures; AMA: Conceptualization, review & editing, writing manuscript first draft; YSR: Supervision and finalized the last version of the manuscript. All authors read and approved the final manuscript.

Funding To Princess Nourah Bint Abdulrahman University Researchers Supporting Project Number (PNURSP2023R28).

Availability of data and materials All data generated or analyzed during the study are included in this article.

Declarations

Conflict of interest Authors declare no conflict of interest directly or indirectly related to the work submitted for publication.

Ethical approval Not Applicable.

Consent to participate Not Applicable.

Consent for publication Not Applicable.

Informed consent Not Applicable.

References

Abdelghany, A.M.: The elusory role of low level doping transition metals in lead silicate glasses. SILICON **2**, 179–184 (2010)

Abdelghany, A.M., Behairy, A.: Optical parameters, antibacterial characteristics and structure correlation of copper ions in cadmium borate glasses. J. Mater. Res. Technol. **9**(5), 10491–10497 (2020)

Abdelghany, A.M., ElBatal, F.H., ElBatal, H.A.: Zinc containing borate glasses and glass-ceramics: search for biomedical applications. Proc. Appl. Ceram **8**(4), 185–193 (2014)

Abo-Mosallam, H.A., Mahdy, E.A.: Crystallization behavior and properties of fluorcanasite–lithium disilicate glasses for potential use in dental application. Ceram. Int. **45**, 21144–21149 (2019)

Abo-Naf, S.M., Khalil, E.S.M., El-Sayed, E.S.M., Zayed, H.A., Youness, R.A.: In vitro bioactivity evaluation, mechanical properties and microstructural characterization of Na_2O-CaO-B_2O_3-P_2O_5 glasses. Spectro Chem. Acta. Part a: Mol. Bio.mol Spec. **144**, 88–98 (2015)

Ahammed, S., Srinivas, B., Shareefuddin, M.: A comparative study on the physical and spectral (optical, EPR and FTIR) properties of NaF-CdO-B_2O_3 and KF-CdO-B_2O_3 glass systems doped with manganese ions. J. Non-Cryst. Solids **594**, 121789 (2022)

Bassam, S.A., Naseer, K.A., Keerthana, V.K., Teresa, P.E., Sangeeth, C.S.S., Mahmoud, K.A., Sayyed, M.I., Alqahtani, M.S., El Shiekh, E., Khandaker, M.U.: Physical, structural, elastic and optical investigations on Dy^{3+} ions doped boro-tellurite glasses for radiation attenuation application. Radiat. Phys. Chem. **206**, 110798 (2023)

Arunkumar, S., Teresa, P.E., Marimuthu, K., Bassam, S.A., Silvia, D.J., Issa, S.A.M., Almisned, G., Tekin, H.O., Alqahtani, M.S., Yousef, E.S.: Scrutinizing the physical, structural, elastic, optical and gamma ray shielding properties of Samarium ions infused Niobium Bariumtelluroborate glasses. Radiat. Phys. Chem. **202**, 110510 (2023)

Baino, F., et al.: Design, selection and characterization of novel glasses and glass-ceramics for use in prosthetic applications. Ceram. Int. **42**(1), 1482–1491 (2016)

Brown, R.F., Rahaman, M.N., Dwilewicz, A.B., Huang, W., Day, D.E., Li, Y.: Effect of borate glass composition on its conversion to hydroxyapatite and on the proliferation of MC3T3-E1 cells. J. Biomed. Mater. Res. A **88**, 392–400 (2009)

Day, D.E., White, J.E., Brown, R.F., McMenamin, K.D.: Transformation of borate glasses into biologically useful materials. Glass Technol. **44**(2), 75–81 (2003)

Divina, R., Teresa, P.E., Marimuthu, K.: Dy^{3+} ion as optical probe to study the luminescence behavior of Alkali lead bismuth borate glasses for w-LED application. J. Alloys Compd. **883**, 1608 (2021)

El-Batal, F.H.: Gamma ray interaction with copper-doped sodium phosphate glasses. J. Mater. Sci. **43**(3), 1070–1079 (2008)

Gallardo-Williams, M.T., Maronpot, R.R., Turner, C.H., Johnson, C.S., Harris, M.W., Jayo, M.J.: Effects of boric acid supplementation on bone histomorphometry, metabolism, and biomechanical properties in aged female F-344 rats. Biol. Trace Elem. **93**, 155–169 (2003)

Goel, A., Tulyaganov, D.U., Kharton, V.V., Yaremchenko, A.A., Ferreira, J.M.F.: The effect of Cr_2O_3 addition on crystallization and properties of La_2O_3-containing diopside glass-ceramics. Acta. Mater. **56**, 3065–3076 (2008)

Hammad, A.H., Marzouk, M.A., ElBatal, H.A.: The Effects of Bi_2O_3 on optical, FTIR and thermal properties of SrO-B_2O_3 glasses. SILICON **8**, 123–131 (2016)

Hench, L.L., et al.: Bonding mechanisms at the interface of ceramic prosthetic materials. J. Biomed. Mater. Res. **5**(6), 117–141 (1971)

Hench, L.L.: Bioceramics: from concept to clinic. J. Am. Ceram. Soc. **74**(7), 1487–1510 (1991)

L.L. Hench, An introduction to bioceramics, 1, World scientific, 1993.

Hoppe, A., Güldal, N.S., Boccaccini, A.R.: A review of the biological response to ionic dissolution products from bioactive glasses and glass-ceramics. Biomaterials **32**(11), 2757–2774 (2011)

Huang, W., Day, D.E., Kittiratanapiboon, K., Rahaman, M.N.: Kinetics and mechanisms of the conversion of silicate (45S5), borate, and borosilicate glasses to hydroxyapatite in dilute phosphate solutions. J. Mater. Sci. Mater. Med. **17**(7), 583–596 (2006)

Jia, W., Zhang, X., Luo, S., Liu, X., Huang, W., Rahaman, M.N.: Novel borate glass/chitosan composite as a delivery vehicle for teicoplanin in the treatment of chronic osteomyelitis. Acta Biomater. **6**(3), 812–819 (2010)

Kamal, H.: Structure and physical properties of silver borate bioactive glasses. Res. J. Pharmaceut. Biol. Chem. Sci. **5**(5), 832 (2014)

Khattari, Z.Y., Al-Ghamdi, H., Alsaif, N.A.M., Rammah, Y.S., Abdelghany, A.M.: Elasto-mechanical and gamma radiation/neutron shielding effectiveness behavior of sodium metaphosphate glasses under different oxidization conditions: effects of zircon ions. Radiat. Phys. Chem. **209**, 110973 (2023)

Kirdsiri, K., Kaewkhao, J., Pokaipisit, A., Chewpraditkul, W., Limsuwan, P.: Gamma rays shielding properties of xPbO:(100–x)B2O3 glasses system at 662 keV. Ann. Nucl. Energy **36**, 1360–1365 (2009)

Krishnamacharyulu, N., Jagan Mohini, G., Sahaya Baskaran, G., Ravi Kumar, V., Veeraiah, N.: Investigation on silver doped B_2O_3–SiO_2–P_2O_5–Na_2O–CaO bioglass system for biomedical applications. J Alloys Compd **734**, 318–328 (2018)
Mahdy, E.A., Ahmed, H.Y., Farag, M.M.: Combination of Na-Ca-phosphate and fluorapatite in wollastonite-diopside glass-ceramic: degradation and biocompatibility. J. Non-Cryst. Solids **566**, 120888 (2021)
Montazerian, M., Zanotto, E.D.: History and trends of bioactive glass-ceramics. J. Biomed. Mater. Res. Part A **104**(5), 1231–1249 (2016)
Moustafa, Y.M., Doweidar, H., El-Damrawi, G.: Utilisation of infrared spectroscopy to determine the fraction of the four coordinated borons in borate glasses. Phys. Chem. Glasses **35**(2), 104–106 (1994)
Nielsen, F.H., Meacham, S.L.: Growing evidence for human health benefits of boron. J. Evid. Base Compl. Alternat. Med. **16**, 169–180 (2011)
Ottomeyer, M., Mohammadkah, A., Day, D., Westenberg, D.: Broad-spectrum antibacterial characteristics of four novel borate-based bioactive glasses. Adv. Microbiol. **6**, 776–787 (2016)
Salinas, A.J., Román, J., Vallet-Regi, M., Oliveira, J.M., Correia, R.N., Fernandes, M.H.: In vitro bioactivity of glass and glass-ceramics of the $3CaO·P_2O_5$–$CaO·SiO_2$–$CaO·MgO·2SiO_2$ system. Biomaterials **21**(3), 251–257 (2000)
Yasaka, P., Pattanaboonmee, N., Kim, H.J., Limkitjaroenporn, P., Kaewkhao, J.: Gamma radiation shielding and optical properties measurements of zinc bismuth borate glasses. Ann. Nucl. Energy **68**, 4–9 (2014)

Publisher's Note Springer Nature remains neutral with regard to jurisdictional claims in published maps and institutional affiliations.

Authors and Affiliations

Hanan Al-Ghamdi[1] · Norah A. M. Alsaif[1] · F. Afaneh[2] · Z. Y. Khattari[2] · A. M. Abdelghany[3] · Y. S. Rammah[4]

✉ Y. S. Rammah
dr_yasser1974@yahoo.com

Hanan Al-Ghamdi
hmalghmdi@pnu.edu.sa

Norah A. M. Alsaif
noaalsaif@pnu.edu.sa

F. Afaneh
afaneh@hu.edu.jo

Z. Y. Khattari
zkhattari@hu.edu.jo

A. M. Abdelghany
a.m_abdelghany@yahoo.com

1 Department of Physics, College of Science, Princess Nourah Bint Abdulrahman University, P.O. Box 84428, 11671 Riyadh, Saudi Arabia

2 Department of Physics, Faculty of Science, The Hashemite University, P. O. Box 330127, Zarqa 13133, Jordan

3 Spectroscopy Department, Physics Research Institute, National Research Centre, 33 ElBehouth St., Dokki, Giza 12311, Egypt

4 Department of Physics, Faculty of Science, Menoufia University, Shebin El-Koom 32511, Egypt